Journal of Drug Delivery Science and Technology 60 (2020) 101980

Contents lists available at ScienceDirect

Journal of Drug Delivery Science and Technology

journal homepage: www.elsevier.com/locate/jddst

Research paper

Development of modified apple polysaccharide capped silver nanoparticles loaded with mesalamine for effective treatment of ulcerative colitis

Gurmandeep Kaur [a], Sachin Kumar Singh [a,*], Rajesh Kumar [a], Bimlesh Kumar [a], Yogita Kumari [a], Monica Gulati [a], Narendra Kumar Pandey [a], K. Gowthamarajan [b,c], Dipanjoy Ghosh [a], A. Clarisse [a], Sheetu Wadhwa [a], Meenu Mehta [a], Saurabh Satija [a], Kamal Dua [d], Harish Dureja [e], Saurabh Gupta [f], Pankaj Kumar Singh [g], Bhupinder Kapoor [a], Nitin Chitranshi [h], Ankit Kumar [a], Omji Porwal [i]

[a] School of Pharmaceutical Sciences, Lovely Professional University, Phagwara, Punjab, 144411, India
[b] Department of Pharmaceutics, JSS College of Pharmacy, JSS Academy of Higher Education and Research, Ooty, Nilgiris, Tamil Nadu, India
[c] Centre of Excellence in Nanoscience & Technology, JSS College of Pharmacy, JSS Academy of Higher Education & Research, Ooty, Nilgiris, Tamil Nadu, India
[d] Discipline of Pharmacy, Graduate School of Health, University of Technology Sydney, Australia
[e] Department of Pharmaceutical Sciences, Maharshi Dayanand University, Rohtak, 124001, Haryana, India
[f] Department of Pharmacology, Chitkara College of Pharmacy, Chitkara University, Rajpura, Punjab, India
[g] Department of Pharmaceutics, National Institute of Pharmaceutical Education and Research, Hyderabad, India
[h] Faculty of Medicine, Health and Human Sciences, Macquarie University, F10A, 2 Technology Place, North Ryde, NSW, 2109, Australia
[i] Department of Pharmacy, Tishk International University, Erbil, Kurdistan Region, Iraq

ARTICLE INFO

Keywords:
Modified apple polysaccharide
Silver nanoparticles
Ulcerative colitis
Mesalamine

ABSTRACT

The objective of study was to develop modified apple polysaccharide (MAP) based silver nanoparticles (AgNPs) loaded with mesalamine (MES) for effective treatment of ulcerative colitis in acetic acid induced rat model. AgNPs were prepared by reducing silver nitrate using MAP solution. The size and zeta potential of AgNPs was 89 ± 3 nm and −16.3 ± 1.54 mV and AgNPs loaded with MES (AgNPs-MES) was 101 ± 9 nm and −14.27 ± 2.16 mV. The dissolution study revealed about 54% drug release after 5 h indicating release of drug at the colonic site. The *in vivo* study was carried out on acetic acid induced ulcerative colitis rats and efficacy of treatment was assessed through evaluation of disease activity index and level of antioxidants as well as tumor necrosis factor-α after 7th and 14th day of induction of colitis. Histopathological evaluation of colonic tissue was also carried out. The results revealed that AgNPs-MES (high dose) provided better therapeutic efficacy for the treatment of UC as compared to its low dose, MES alone, MES-MAP, AgNPs alone and MAP alone. It was concluded that MAP based AgNPs loaded with MES were successfully formulated and found to be effective in treating ulcerative colitis.

1. Introduction

The overall prevalence rate for inflammatory bowel disease (IBD) has been reported to be 6.8 million and among them the prevalence rate of ulcerative colitis (UC) is high [1]. The high rates are reported in the industrial areas [2–9]. There are several treatments till now attempted to treat UC [10–13], however, they succeeded up to some extent only. So, the need of therapy for treatment of UC has become very important nowadays. UC's treatment options can be categorized into two attempts, first, that alters the presumed pathogenesis of UC and second, that controls the severity and symptoms of UC. Many patients experience the relapse of UC and proliferation of disease during their clinical course. Its therapy has been divided as maintenance therapy, induction therapy, treatment for refractory disease followed by surgery. Out of these, efficacious acute therapy and safe maintenance therapy play important role in treatment of UC. There are three main classes of agents that have been used for treatment of UC. These include corticosteroids, immunomodulators and mesalamine (MES). MES is also popularly known as 5-aminosalicylic acid (5-ASA). Antidiarrheal and antispasmodic preparations have also been reported to control the severity and symptoms of UC. Other preparations like antipsychotic, antidepressants and sedatives are not recommended as a daily dose but their low doses are

* Corresponding author. School of Pharmaceutical Sciences, Lovely Professional University, Phagwara, 144411, Punjab, India.
E-mail addresses: singhsachin23@gmail.com, sachin_pharma06@yahoo.co.in, sachin.16030@lpu.co.in (S.K. Singh).

https://doi.org/10.1016/j.jddst.2020.101980
Received 6 May 2020; Received in revised form 21 July 2020; Accepted 30 July 2020
Available online 9 August 2020

recommended to ameliorate symptoms in UC patients [14].

Till date, MES is first line drug for UC. Various colon targeted drug delivery systems are previously reported for MES. These include, guar gum and Eudragit S100 coated mini tablets [11], hydroxy propyl methyl cellulose E−15 and Eudragit S100 based press-coated tablets [15], chitosan/Eudragit S100 based mesalamine microspheres [16], guar gum/xanthan gum based microspheres [17]. However, these formulations were reported to have certain limitations such as premature drug release during diseases state in case of pH dependent delivery system as the pH of GIT changes [13,18,19]and incomplete drug release in case of polysaccharide-based delivery systems due to loss of gut microflora [20,21]. In recent years, several attempts have been made to develop oral formulation of MES along with other drugs/probiotics/prebiotics to get successful treatment [11,13,19,20,22]. This approach has been taken into account because imbalance of the colonic micro flora is one of the major causes for the disease.

In recent years, silver nanoparticles (AgNPs) and modified apple polysaccharide (MAP) have been explored for treating UC due to their anti-inflammatory properties [23–25]. During UC, inflammation occurs due to the release of prostaglandin and chemotactic substances like interleukin-1 (IL-1), complement factors, TNF-α and tumor growth factor-β (TGF-β). AgNPs are able to suppress the activity of these inflammatory markers [25].

In colorectal cancer cells, MAP induces apoptosis via caspase-dependent mechanism.

MAP is also known to inhibit lipopolysaccharide (LPS)induced toll-like receptor 4 (TLR4) as well as Nuclear Factor (NF)-κB pathway, thereby inhibiting metastatic activities [11,26].

Recently MAP has been reported to produce gold nanoparticles by reduction of aurochloric acid. Successful oral delivery of insulin was achieved by loading insulin with MAP capped gold nanoparticles [27]. Taking a cue from this, AgNPs were prepared by using the method of reduction of silver nitrate employing MAP as reducing agent. The prepared MAP capped AgNPs are loaded with MES (AgNPs-MES) and explored to evaluate their potential to treat ulcerative colitis in acetic acid induced rat model. MES and AgNPs are expected to provide anti-ulcer and anti-inflammatory effect. MAP is expected to provide dual benefits i.e. being a polysaccharide it will be able to provide site specific release to intestine/colon by delaying the complete release of drug at upper gastrointestinal (GI) tract [13,18,28–33] and anti-inflammatory effect against UC [11]. Hence, this combination is expected to achieve multiple benefits such as, better absorption and therapeutic efficacy of MES at much lower doses due to its loading with AgNPs to treat UC.

2. Experimental

2.1. Materials

Apples, the fruit of plant *Malus domestica* (Family: *Rosaceae*) were purchased from authorized supplier in Punjab, India. Silver nitrate ($AgNO_3$) was procured from BB Pvt. Ltd., New Delhi, India. Sodium citrate and MES were procured from Hi Media Pvt. Ltd. Ethanol, sulphuric acid, copper acetate, aerosil (A-200), hydroxy furfural acetate, disodium hydrogen phosphate, potassium dihydrogen phosphate and trehalose were purchased from central drug house (CDH) Pvt. Ltd., New Delhi, India. Micro crystalline cellulose, lactose, hydrochloric acid, potassium chloride and acetic acid were purchased from Lobacheime, Mumbai, India.

2.2. Development of calibration curve for silver nitrate ($AgNO_3$)

$AgNO_3$ (100 mg) was weighed and transferred into 10 mL of standard volumetric flask and dissolved in 10 mL of water to obtain a concentration of 10 mg/mL of stock solution. Then 1.94 g of solution of potassium chromate (K_2CrO_4) was prepared in 10 mL of water and 2–3 drops of this solution was added into stock solution. Aliquots of standard solution ranging from 5 to 25 μg/mL were transferred into series of 10 mL of volumetric flasks. The absorbance of prepared dilutions was measured at 285 nm.

2.3. Preparation of MAP solution

Apples (500 g) were cut and crushed in a mortar pestle. Crushed apples were taken in a 500 mL glass beaker and soaked overnight in ethanol to remove fatty materials. This dispersion was boiled 3 times for 8 h each time with absolute ethanol for 24 h to extract the components dissolved in ethanol. Ethanol was removed and solid mass was dried in an oven at 60 °C for 8 h. The residue was boiled in water at 100 °C three times for 8 h for extraction of polysaccharides. The aqueous extracts were combined and mixed with concentrated ethanol solution (75 mL/L) to precipitate the fraction that were rich in polysaccharide. This was followed by removal of proteins by freeze-thawing method. The MAP was obtained through dialysis. Dialysis was carried out by keeping the apple solution (5 mL) inside the dialysis bag having molecular-weight cut off (MWCO) limits of 2000 Da. The membrane fixed with a dialysis tubing closure in the dialysis chamber filled with 200 mL of phosphate buffer saline (dialysate) was kept on a magnetic stirrer and stirred at 50 rpm. The study was carried out at room temperature for 2 h and then the dialysate was replaced with fresh one. The dialysis was carried out for another 2 h and once again the old dialysate was replaced with fresh one. Then the study was continued till 72 h. The dialyzed sample was concentrated. The concentrated samples were lyophilized using Freeze dryer (EBT-12 N, Chennai, India). The obtained residue of MAP (10 mg) was hydrolyzed with 1 mL of 2 N trifluoroacetic acid at 105 °C for 8 h. Dried sample was neutralized using 3 N sodium hydroxide maintained at pH 7.0 [26,34]. The yield (%) of MAP was calculated as the ratio of the quantity of liquid MAP obtained after the entire extraction procedure divided by the initial amounts of raw apples taken for extraction and the ratio was multiplied by hundred.

Ten different aqueous solutions of MAP with strengths ranging from 0.5 to 5% v/v with an increment of 0.5, were prepared and kept undisturbed for 30 min.

2.4. Preparation of AgNPs

For the preparation of AgNPs, 5 mM solution of $AgNO_3$ was added to 10 mL aqueous solution of MAP of varying concentrations (0.5%v/v-5% v/v). The prepared solutions were stoppered and kept in dark for 1 h. After this, slight change in color from colourless to light brown was observed in all the concentrations. All the solutions were scanned using UV–Visible spectrophotometer to confirm the synthesis of AgNPs. For the evaluation of stability and selection of final formulation, the UV scan of the prepared solutions was taken in the wavelength range of 400–800 nm for 3 consecutive days.

2.5. Loading of MES in AgNPs

2.5.1. Development of calibration curve of MES

MES (10 mg) was weighed and transferred into 10 mL of standard volumetric flask. The solution was further diluted into 10 mL of 0.1 N hydrochloric acid (HCl) to obtain the concentration of 100 μg/mL. For calibration curve of MES, different aliquots were taken from the above solution and solutions of different concentrations (4, 8, 12, 16 and 20 μg/mL) were prepared in 10 mL of HCl. The absorbance was recorded at the wavelength of 324 nm and the calibration curve for MES was plotted between the concentrations versus absorbance.

2.5.2. Loading of MES to AgNPs (AgNPs-MES)

It is important to note that among all the prepared AgNPs, nanoparticles prepared using 3.5% v/v of MAP were found more stable, hence, this solution was selected for further studies (*please see results and discussions*). This solution (10 mL) was taken in 50 mL glass beaker and

Table 1
Treatment groups and their doses used in the study.

Groups	Treatment	Animals Used	Dosage and Route of administration
1	Normal saline	6	0.9% w/v, 0.2 mL/rat, intracolonic administration +0.5% w/v CMC, p. o.
2	Acetic Acid (AA)	6	6% v/v AA for 15 s, 0.2 mL, intracolonic administration
6% v/v AA for 15 s, 0.2 mL has been administered to all the rats of group 3 to 9 through intracolonic administration followed by their individual treatments			
3	MAP	6	3.5% v/v, p.o.
4	MES	6	23 mg/kg (suspended in 0.5% w/v CMC), p.o.
5	AgNPs (low dose)	6	1 mg/kg (suspended in 0.5% w/v CMC), p.o.
6	AgNPs (high dose)	6	4 mg/kg (suspended in 0.5% w/v CMC), p.o.
7	MAP + MES	6	3.5% v/v, p.o.+23 mg/kg (suspended in 0.5% w/v CMC), p.o.
8	AgNPs-MES[a] (low dose)	6	1 mg/kg + 23 mg/kg (suspended in 0.5% w/v CMC), p.o.
9	AgNPs-MES[a] (High dose)	6	4 mg/kg + 23 mg/kg (suspended in 0.5% w/v CMC), p.o.

[a] Dose of MES is kept constant in group 8 and group 9.

23 mg of MES was dissolved in it. The solution was kept aside for 5 h for loading of AgNPs with MES (AgNPs-MES). To separate the free drug from the drug loaded AgNPs, dialysis was carried out by keeping the AgNPs-MES solution (5 mL) inside the dialysis bag having MWCO limits of 2000 Da. The membrane fixed with a dialysis tubing closure in the dialysis chamber filled with 200 mL of phosphate buffer saline (dialysate) was kept on a magnetic stirrer and stirred at 50 rpm. The study was carried out at room temperature. During the dialysis process, at every 1 h, 1 mL of dialysate was taken out and analyzed for drug concentration by recording absorbance at 324 nm. The withdrawn medium was replaced with 1 mL of fresh media. This process was continued till the drug concentration showed no significant change, which indicated the dialysis has reached a state of equilibrium. The encapsulation efficiency (%) of MES in the AgNPs was calculated indirectly by measuring the concentration of free drug present in the solution and dividing it with total concentration of MES added in the AgNPs dispersion using the formula given in Eq. (1).

$$\%\ Encapsulation\ efficiency = \frac{Concentration\ of\ free\ MES\ present\ in\ AgNPs\ -\ MES\ dispersion}{\text{Total concentration of MES added in the } AgNPs\ -\ MES\ dispersion} 100 \quad \text{Eq.(1)}$$

2.6. Characterization of synthesized AgNPs-MES

2.6.1. Surface plasmon resonance (SPR)

SPR for final formulation of AgNPs and AgNPs-MES was recorded in the range of 200–600 nm to confirm the formation of AgNPs and AgNPs-MES. The overlay of both the spectrum was recorded.

2.6.2. Dynamic light scattering (DLS)

Size distribution, polydispersity index and zeta potential of the prepared AgNPs and AgNPs-MES were measured using Zetasizer ZS90. A laser beam of 50 mV was projected on the plastic sample cells at an angle of 90°. Samples (1 mL) were diluted to 10 mL using distilled water and analyzed. The analysis was carried out in triplicate and their mean value was recorded [27].

2.6.3. Transmission electron microscopy (TEM)

The shape of AgNPs and AgNPs-MES was analyzed through TEM (JEM 1010; JEOL, Tokyo, Japan). Phosphotungstic acid of 2% w/v concentration was used to stain the formulations. Afterwards they were applied on copper grid and allowed to dry in air. Images were then recorded at a scale bar of 200 nm [27,35].

2.7. Release study in bio-relevant media

The release study was performed for MES and AgNPs-MES in medium containing rat caecal contents (RCC) as well as in medium without rat caecal content (WRCC) using paddle apparatus. Speed of paddle was kept at 50 ± 4 rpm and temperature of medium was kept at 37 ± 0.5 °C. Samples (10 mL) were added to dissolution vessels. First step of the study was performed in 200 mL of 0.1 N HCl for 2 h. At the end of second hour, 700 mL of phosphate buffer (0.2 M; pH 6.8) was added to the same medium and the pH of medium was adjusted to 6.8 using sodium hydroxide solution (0.2 M). The confirmation of pH throughout the study was done using pH meter. The total volume of medium became 900 mL. Twenty minutes before the completion of 5 h, three rats were sacrificed and abdominal incision was done to isolate their caecal contents. These caecal contents (15 g) were transferred into 300 mL of phosphate buffer. From this, 100 mL rat caecal content solution (5% w/v) was transferred into each of the three dissolution vessels. It is important to note that addition of 4–5% w/v of rat caecal contents in dissolution medium is recommended to achieve sufficient number of microbes/enzymes to degrade the polysaccharide matrix/coat [18,21,36]. The final volume of vessel was adjusted to 1000 mL. The study was continued for 24 h with constant purging of CO_2 for achievement of anaerobic conditions. After every 1 h, samples (5 mL) were withdrawn and replaced by 5 mL of blank solution to maintain sink conditions up to 24 h. The samples were evaluated by UV–Visible spectrophotometer at the wavelength of 324 nm.

2.8. In vitro cell line toxicity study

Cytotoxicity assays was carried out by 3-(4,5 dimethyl thiazole-2 yl)-2,5-diphenyl tetrazolium bromide (MTT) assay using Caco-2-cells. Cell culture was centrifuged and the cell density of the suspension was adjusted to 1.0 × 10^5 cells/mL. Dulbecco's Modified Eagle Medium (DMEM) containing 10% FBS was used as the culture medium. An amount of 100 μL of this diluted inoculum (approximately 10,000 cells/well) was added per well of a 96 well flat bottom micro titre plate. Serial dilution of $AgNO_3$, AgNPs and AgNPs-MES were prepared in the range from to 4 μg/mL to 250 μg/mL. After 24 h, the cells were centrifuged, supernatants were removed and the pellets were suspended with 100 μL of the test samples of different strengths prepared in maintenance media. These plates were kept in humidified incubator at 37 °C for 48 h with a 5% CO_2 atmosphere and examined microscopically every 24 h. After 48 h, serial dilutions of these samples were prepared, centrifuged and the pellets were re-suspended with 20 μL of MTT (2 mg/mL) in phenol red free minimum essential medium (MEM-PR). The plates were gently shaken and incubated for 15 min at 37 °C in 5% CO_2 atmosphere. A quantity of 100 μL of DMSO was added and the plates were gently shaken to solubilize the formed formazan. Absorbance was measured at a wavelength of 540 nm using a micro plate reader. The percentage cell viability was calculated using equation (2) while the strength of the sample required to inhibit cell growth by 50% was calculated by plotting

Table 2
Scoring system for stool consistency and % weight loss.

Score	Stool consistency	% Weight loss
0	Normal	0 or gain
1	Normal	1–4.9
2	Loose	5–9.9
3	Loose	10–20
4	Diarrhea	20–25
5	–	25–30

dose response curve.

$$\%\ Cell\ viability = Mean\ optical\ density\ of\ individual\ test\ solution \div Mean\ optical\ density\ of\ standard\ solution \quad \text{Eq.(2)}$$

2.9. In vivo study animal study for treatment of UC

The study was carried out using 54 animals with six animals in each of the nine groups as shown in Table 1. Rats (Sprague Dawley) of either sex, weighing between 250 and 300 g, were purchased from NIPER, Mohali, India. The study was approved by Institutional Animal Ethics Committee (IAEC Protocol Number: LPU/IAEC/2019/45). The animals were kept under light and dark cycles of 12 h at 25 ± 2 °C for 10 days prior to initiation of study and fed with standard rat chow diet and water ad libitum [11].

2.9.1. Induction of colitis and treatment of UC

The UC was induced to rats by intracolonic administration of 0.2–0.3 mL of acetic acid (AA) using propylene tube (0.2 mm diameter). The tube was dipped in glycerine and inserted through rectum up to a length of 7–8 cm in colon. After administration of AA, animals were held in supine Trendelenburg position for 15 s [37].

2.9.2. Treatment protocol

Rats of Group 1 were administered 1 mL of normal saline orally for 14 days. Rats of Group 2–9 were treated with AA as mentioned in 2.10.1 for induction of UC. Group 2 rats did not receive any treatment for next 14 days after induction of UC, whereas, after induction of UC (i.e. 72 h) the rats of other groups were given the respective treatment as mentioned in Table 1 for 14 days.

2.9.3. Estimation of UC

2.9.3.1. Disease activity index (DAI)

2.9.3.1.1. Stool consistency. The consistency of stools of each animal of each group was observed on the 0th, 7th and 14th day of study. The DAI was determined by referring the scale of stool consistency as shown in Table 2 [11,13,17,38].

2.9.3.1.2. wt loss. Weight loss for each animal of each group was observed on 0th, 7th and 14th day of the study, DAI was determined by adding the scale of the weight loss as presented in Table 2 [17,38].

2.9.3.2. Estimation of reduction in glutathione (GSH) levels. GSH was estimated by homogenizing colonic tissue (720 μL) with 5% w/v trichloroacetic acid (TCA). The homogenate was centrifuged at 10,000 *g* for 5 min to precipitate tissue matrix. The supernatant was mixed with Ellman's reagent/5,5′ dithio bis (2 nitrobenzoic acid) and their absorbance was recorded at 412 nm. A calibration curve was plotted using different strengths of standard GSH solution. The concentration of GSH present (nmol/mg protein) in tissue homogenate was calculated using the regression equation obtained from calibration curve [39].

2.9.3.3. Estimation of thiobarbituric acid reactive substances (TBARS). TBARS is used as a marker for lipid peroxidation. Its levels in the samples were calculated by estimating the strength of MDA. To calculate this, three different solutions *viz* 0.1 M Tris-HCl buffer (pH 7.4), thiobarbituric acid (TBA, 0.67% w/v) and 10% w/v TCA were prepared. Colonic tissue homogenate (1 mL) was mixed with 1 mL of Tris-HCl in a test tube centrifuged at 1000 *g* for 10 min and supernatant (1 mL) was mixed with TBA solution. The mixture was heated at 50 °C for 2 min and cooled. To the cooled solution, distilled water (1 mL) was added and absorbance was determined at 532 nm [40]. The concentration of TBARS was calculated in mMoles MDA/mg protein using Equation (3).

$$3 \times optical\ density\ of\ sample \div 0.156 \times mg\ protein\ /\ 0.2 = nmoles\ ofMDA/\ mg\ protein \quad \text{Eq.(3)}$$

2.9.3.4. Estimation of myeloperoxidase (MPO). Colonic tissue sample of 5 cm length from each rat was isolated and cleaned in saline cooled in saline, blotted dried and then weighed. The weighed samples were then subjected to homogenization by using tissue homogenizer (Remi RQ 127 a, Vasai, Mumbai, India). The process of homogenization was performed in 10 mL of 50 mM potassium phosphate buffer cooled in ice, having pH 6.0 and containing 0.5% w/v hexadecyl trimethyl ammonium bromide (HETAB). The prepared homogenates were sonicated for 10 min using ultra sonicator (Loba life, Mumbai, India). The sonication was followed by the process of centrifugation on a cooling centrifuge (M – 1214, Remi, Vasai, Mumbai, India) at 12000 g for 20 min at 4 °C. A sample of 0.1 mL from the supernatant was withdrawn from each tube and mixed with 2.9 mL of phosphate buffer (pH 6.0) containing 0.0005% v/v H_2O_2.

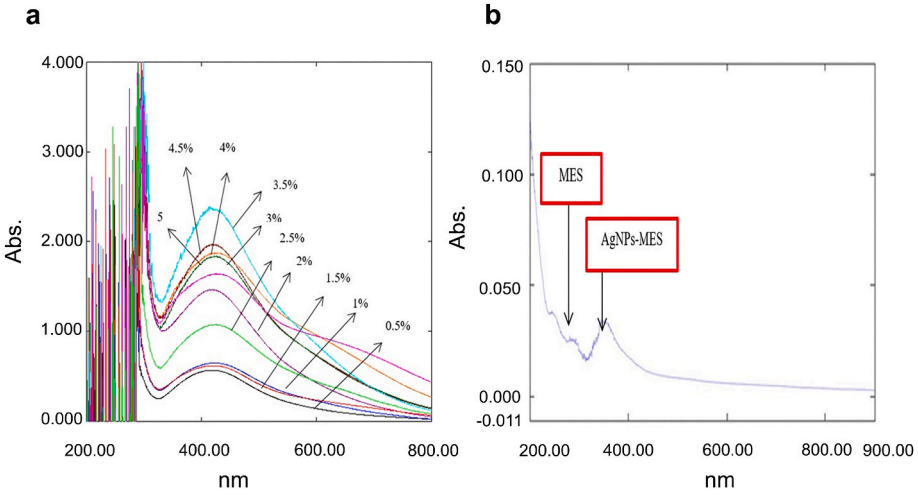

Fig. 1. SPR of a. AgNPs prepared using various concentrations of MAP; b. AgNPs-MES.

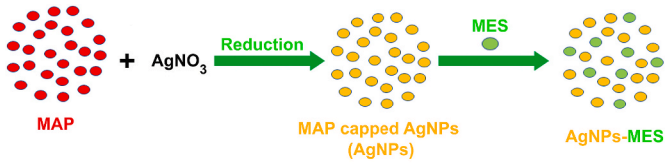

Fig. 2. Schematic representation of preparation of AgNPs-MES.

UV spectrophotometer was used to measure the change in absorbance per minute (Shimadzu UV 1800, Japan) at 460 nm. A single unit of MPO is defined as the change in absorbance per minute by 1.0 unit at room temperature. It was calculated by using equation (4) [41].

$$MPO\ activity\ (U/g) = X \div Weight\ of\ tissue\ taken \quad \text{Eq.(4)}$$

where, X = 10 × change in absorbance/minute/volume of supernatant taken in final reaction.

2.9.3.5. Estimation of superoxide dismutase (SOD). Isolated colonic tissue was homogenized in a mixture of sodium pyrophosphate buffer (1.2 mL), 0.1 mL of phenyl methane sulphonyl fluoride (PMSF), nitro blue tetrazolium (0.3 mL) and enzyme preparation (0.2 mL). The total volume was adjusted to 2.8 mL using water. For initiating the reaction, Nicotinamide Adenine Dinucleotide Hydrogen (2 mL) was added to the mixture and incubated for 90 s. The reaction was stopped by addition of 1 mL of glacial acetic acid. To this, n-butanol (4 mL) was added and kept aside for 10 min. This mixture was centrifuged at 5000 *g* for 10 min and the intensity of the chromogen present in the butanol layer was measured at 560 nm "A single unit of enzyme activity can be defined as the net amount of enzyme required to give an inhibition of 50% of NBT reduction in a 60s" [42].

2.9.3.6. Estimation of tumor necrosis factor-α (TNF-α). On 7th and 14th day, isolated colonic tissue was added to solution containing mixture of phosphate buffer solution, PMSF and protease inhibitor and homogenized for 15 min using tissue homogenizer at 5000 rpm for 15 min. The homogenate was sonicated and sodium lauryl sulphate was added to it. Afterwards, the homogenate was kept in ice cold water for 30 min. It was sonicated again and centrifuged at 10,000 *g* for 10 min at 4 °C. The supernatant was separated and level of TNF- α was estimated using ELISA kits from eBiosciences (USA) [40].

2.9.3.7. Histopathological examination. The colonic tissues (4 cm length) were excised on seventh and fourteenth day. These tissues were weighed and fixed in 10% v/v of neutral buffered formalin solution for 24 h. Transverse sections of these tissue were embedded in paraffin blocks. Staining of isolated tissue was done using haematoxylin-eosin (HE) and subjected to histopathological examination by qualified pathologist [13]. Imaging was done using x 40 lens. The parameters used to assess colonic tissue's damage include crypt's loss, loss of integrity of mucosal epithelium, and extent of inflammation.

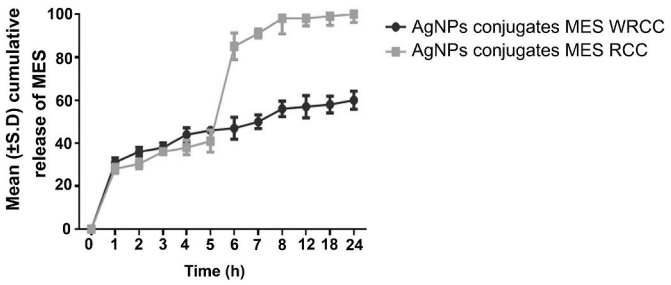

Fig. 4. *In-vitro* drug release study of AgNPs-MES in RCC and WRCC.

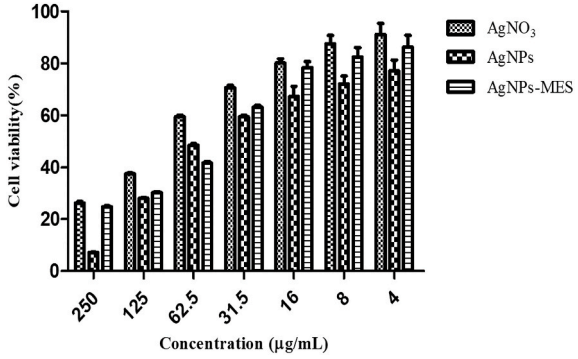

Fig. 5. Results of cell viability for AgNO3, AgNPs and AgNPs-MES at different concentrations.

2.10. Statistical analysis

The obtained results from the experiment were expressed as mean ± SD. The graphs were plotted using Graph Pad Prism version 7.0 (Graph Pad software INC., CA, USA). The results were compared using analysis of variance and Student 't' test. The $P < 0.05$ (wherever, applicable) value indicated significant difference in the results. The similarity factor (f2) was calculated using model independent analysis and value between two dissolution profiles above 50 indicated similarity between two profiles [43].

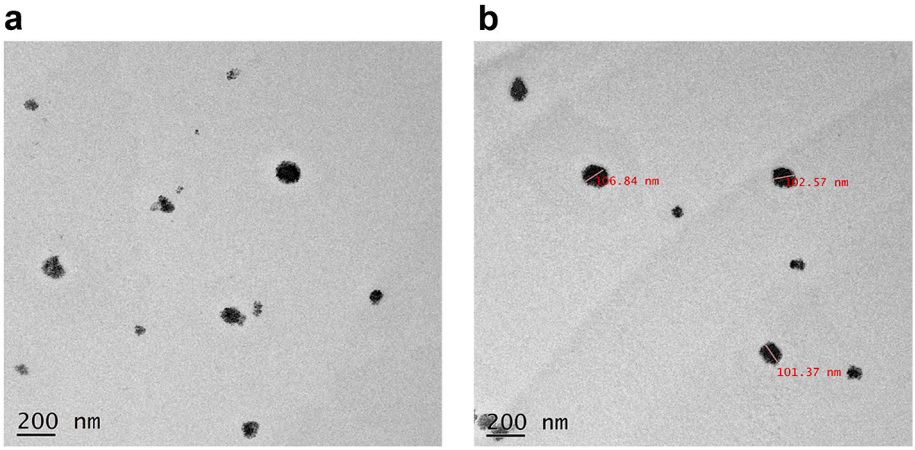

Fig. 3. TEM images of A. MAP-capped AgNPs (AgNPs) and B. AgNPs-MES.

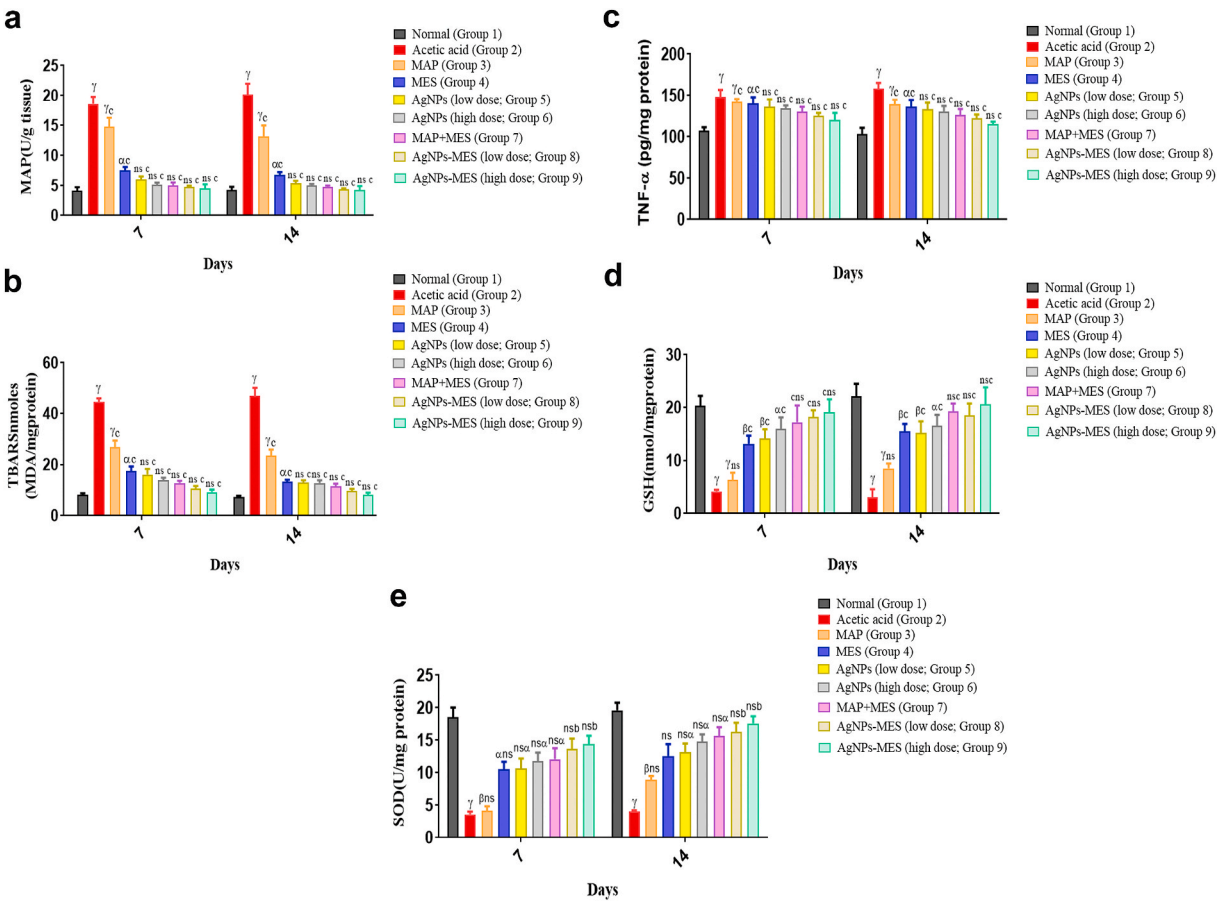

Fig. 6. Results of a-MPO, b-GSH, c-SOD and d-TBARs. Data analysis were done by one-way analysis of variance, followed by Bonferroni's multiple comparison test. Results are expressed as mean ± SEM (n = 6), α = P < 0.05, β = P < 0.01, y = P < 0.001, ns = not significant as compared to the normal control group; a = P < 0.005, b < P.01, c = P < 0.001 compared to the experiment control group; ns* = not significant as compared to the experimental control group.

3. Results and discussions

The calibration curve of $AgNO_3$ was recorded and it was found linear in the range of 5–25 μg/mL as the coefficient regression (R^2) was found to be 0.992. The extracted MAP was characterized for density, molecular weight, polysaccharide content. The density of prepared MAP solution was found to be (1.03 g/mL) which was in agreement with our previously published work [44]. The yield of MAP was 55%. Further, the major components of MAP were galactose and galacturonic acid. The molecular weight of MAP was 2500–3000 Da and the amount of sugar was more than 85% and protein content was less than 3%. These were found in concordance with previously published research works [24, 26].

3.1. Preparation of AgNPs

The AgNPs prepared exhibited their absorbance maxima i.e. SPR at 400 nm (Fig. 1a). This absorption at 400 nm is due to excitation of surface plasmon vibration by colloidal silver nanoparticles [45,46]. The results indicated maximum absorbance of AgNPs containing 3.5% v/v MAP indicating maximum formation of AgNPs at this concentration as compared to those formed using other concentrations of MAP [47]. Hence, this formulation was selected for conjugating MES.

3.2. Characterization of optimized AgNPs-MES

3.2.1. Encapsulation efficiency

It is important to note that the absorbance maxima (SPR) of AgNPs-MES nanoparticles was found at 383 nm (Fig. 1b). The encapsulation efficiency of MES in AgNPs was found to be 93 ± 3.21%. A decrease in intensity of absorbance maxima and blue-shift in SPR of AgNPs from 400 nm to 383 nm was observed after loading of MES which could be attributed to physical interaction and increased electrostatic repulsions between the colloidal silver nanoparticles and mesalamine particles [45, 46,48].

3.2.2. Particle size and zeta potential

The zeta potential for AgNPs and AgNPs-MES was found to be −16.3 ± 1.54 mV and −14.27 ± 2.16 mV. Mean particle of AgNPs and AgNPs-MES was found to be 89 ± 3 nm and 101 ± 9 nm, respectively. The polydispersity index was found to be 0.577 ± 0.08 and 0.352 ± 0.065 for AgNPs and AgNPs loaded MES, respectively. The p-value was found above 0.05 for zeta potential, particle size and polydispersity index of AgNPs and AgNPs-MES indicated absence in any significant change in these properties after loading of MES to the AgNPs. The results indicated negative charge on zeta potential of AgNPs-MES because of capping of AgNPs by MAP. MAP being a polysaccharide, possesses negative charge on it. A reduction in negative charge of zeta potential was observed upon loading of MES with AgNPs (AgNPs-MES). The complete scheme of formation of AgNPs-MES is shown in Fig. 2. The figure illustrates the adsorption of MAP onto the surface of AgNPs and embedment of MES in the matrix of MAP-capped AgNPs. The slight increase in size of AgNPs was observed upon loading of MES.

The TEM images of MAP-capped AgNPs and AgNPs-MES are shown in Fig. 3. The images revealed formation of spherical nanoparticles. The average size obtained from TEM analysis for AgNPs was 91.75 ± 3.21 nm and AgNPs-MES was 103.59 ± 4.02 nm, whereas, the size obtained from DLS studies was 89 ± 3 nm for AgNPs and 101 ± 9 nm for AgNPs-

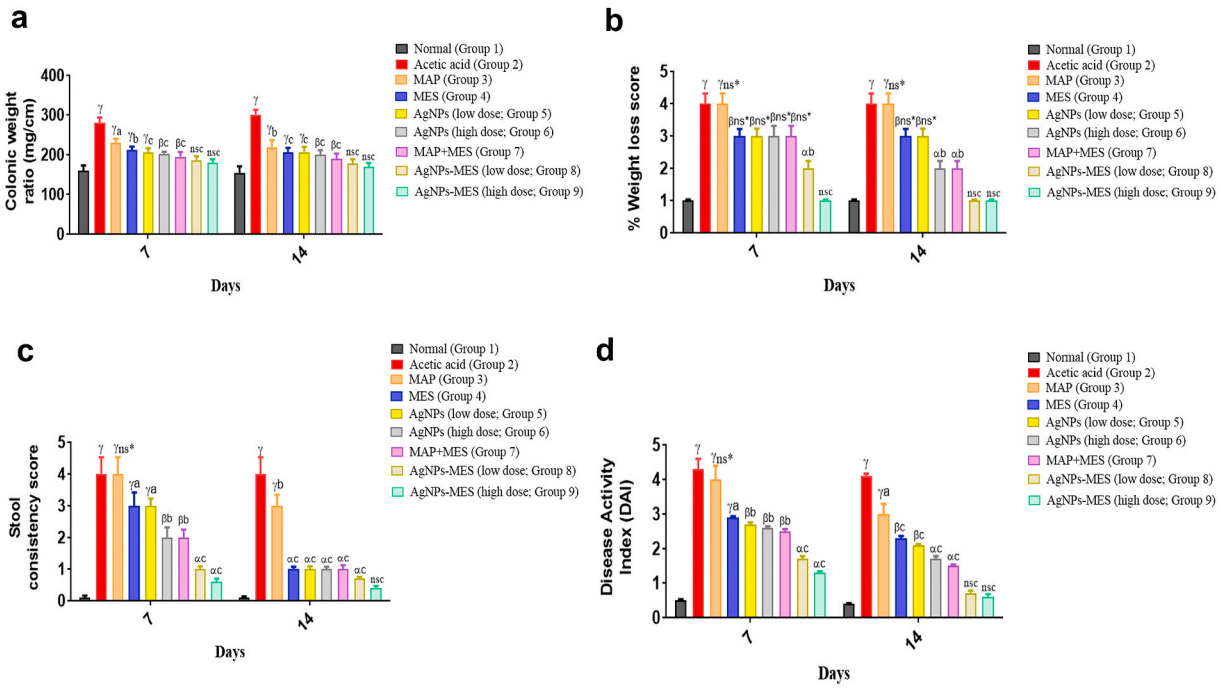

Fig. 7. Results of a. colonic weight; b. %weight loss; c. stool consistency; d. overall DAI. Data analysis were done by one-way analysis of variance, followed by Bonferroni's multiple comparison test. Results are expressed as mean ± SEM (n = 6), α = P < 0.05, β = P < 0.01, y = P < 0.001, ns = not significant as compared to the normal control group; a = P < 0.005, b < P.01, c = P < 0.001 compared to the experiment control group; ns* = not significant as compared to the experimental control group.

MES. Hence, a non-significant difference ($p > 0.05$) in results of particle size indicated a better correlation between the results of particle size obtained from DLS and TEM studies. The images also showed increase in size upon loading of AgNPs with MES (Fig. 3).

3.2.3. *In vitro drug release study*

AgNPs-MES were subjected for drug release studies for 24 h in a medium containing RCC as well as WRCC. The results revealed of AgNPs-MES subjected in WRCC revealed only 46 ± 2% release of MES from the formulation in the first 5 h. This indicated slow and sustained diffusion of MES (about 50% release) from the matrix of polysaccharide (MAP) for first 5 h i.e. upper GIT [49,50]. The results indicated that 54% release of MES got restricted in the upper GIT because of drug loaded nanoparticles entrapped in the matrix, of MAP, which is a polysaccharide (Fig. 4). Even after 24 h, the maximum drug release was found to be only 60 ± 2%. This was due the unavailability of microbiota that could have degraded the polysaccharide matrix. Whereas, in the case of formulation subjected to medium containing RCC, the drug release from AgNPs-MES was found 41 ± 5.18% in first 5 h (i.e. about 59% restriction of drug release in upper GIT). Upon addition of the rat caecal content (RCC) at the end of the 5th h, a sudden rise in the drug release was observed at the end of 6th h (85 ± 3%). Almost complete drug got released (98 ± 2%) within 12 h of the study and at the end of 24 h the release was found to be 100 ± 9%. It is important to note that in both the cases, the drug release profiles were similar till first 5 h ($f2 = 95$; $p = 0.70$), indicating sustained release pattern. When the formulation came in contact of RCC (i.e. after 5 h), an immediate burst release of MES was observed in case of formulation subjected in medium containing RCC as compared to the one in which RCC was not added ($f2 = 19$; $p < 0.0001$).

3.2.4. *In vitro cell line toxicity study*

More than 86% of the cells were found to be viable at concentration of 4 μg/mL for AgNPs-MES while 77% of the cells were viable in case of treatment with AgNPs alone (Fig. 5). Metallic nanoparticles are known to cause cellular toxicity but in the present study cellular protection for more than 50% cells in case of AgNPs could be due to presence of MAP which is known to possess anti-ulcer and antioxidant activity [11]. Further enhanced cellular protection was observed in case AgNPs-MES as that of AgNPs alone due to anti-ulcer and anti-inflammatory action of MES. It is important to note that the dose of AgNPs used in the present study was 4 mg/kg body weight of rats. This means 1 mg dose for 250 g of rats has been administrated. This indicated 4 μg/g (equivalent to 4 μg/mL) of AgNPs have been administrated which are found to be safe in cell line studies.

3.2.5. *Results of antioxidant and inflammatory markers*

The efficacy of AgNPs-MES was evaluated through different pharmacodynamics studies conducted on acetic acid induced UC in rats. Various parameters like MPO, SOD, GSH, TBARSs and TNF-α were estimated. MPO is an enzyme which found in the neutrophil and used as an indicator for neutrophil infiltration of the tissues. This activity is also used as a marker for the inflammatory process in the intestine. The results of MPO obtained from samples collected on 7th and 14th day (Fig. 6a) indicated significantly higher MPO values ($p < 0.05$) in group 2 as compared to all the other groups. This was due to the fact that the rats of group 2 received no treatment after induction of UC and rest of the UC induced groups (groups 3 to 9) who received treatment, showed recovery of different extent based upon the efficacy of their treatment. The maximum recovery (i.e. decrease in MPO level) was observed in rats of group 9 who received high dose of AgNPs-MES, followed by group 8 who received low dose of AgNPs-MES. The treatment efficacy of group 8 and 9 was found better as compared to rats of group 5 and 6. This clearly indicated increase in treatment efficiency of AgNPs upon their co-administration with MES (group 8 and 9). Furthermore, it is important to note that the dose of MES was same for rats of group 8 and 9, hence, the improved results with rats of group 9 as that of group 8 and group 6 as that of group 5 was due to increase in dose of AgNPs. This clearly indicated potential of AgNPs as anti-ulcer agent. The results also indicated that there was no significant difference in the MPO activity of

Table 3
Histopathology report of transverse section of colonic tissue.

Group 1	Normal control (NC)	7th (A1)	Normal looking mucosa with no lesions of pathological significance
		14th (A2)	Normal looking mucosa with no lesions of pathological significance
Group 2	Experimental control (EC)	7th (B1)	Diffused active colitis; superficial erosions, stromal edema, dense acute and chronic inflammatory cells infiltrate with widely ulcerating mucosa
		14th (B2)	Diffused active colitis; superficial erosions, stromal edema, dense acute and chronic inflammatory cells infiltrate with widely ulcerating mucosa but with less severity
Group 3	MAP solution	7th (C1)	Fewer rise in number of goblet cells, slight disruption of epithelial lining; low neutrophilic infiltration
		14th (C2)	Very slight disruption of epithelial lining; negligible neutrophilic infiltration.
Group 4	Mesalamine	7th (D1)	Damage of crypt cells; rise in number of goblet cells, disruption of epithelial lining; neutrophilic infiltration
		14th (D2)	Slight damage in the crypt cells; negligible surface epithelial loss, neutrophilic infiltration
Group 5	AgNPs (Low Dose)	7th (E1)	Moderate neutrophilic infiltration; negligible disruption of epithelial lining.
		14th (E2)	Low neutrophilic infiltration; negligible disruption of epithelial lining.
Group 6	AgNPs (High Dose)	7th (F1)	Low neutrophilic infiltration; negligible disruption of epithelial lining.
		14th (F2)	Negligible neutrophilic infiltration; negligible disruption of epithelial lining.
Group 7	MAP + Mesalamine	7th (G1)	Low neutrophilic infiltration; negligible disruption of epithelial lining.
		14th (G2)	negligible neutrophilic infiltration; negligible disruption of epithelial lining.
Group 8	AgNPs-MES (Low Dose)	7th (H1)	Absence of acute inflammation, signs of neutrophilic infiltration; a little disruption of epithelial lining
		14th (H2)	Complete absence of acute inflammation, absence of disruption in epithelial cells.
Group 9	AgNPs-MES (High Dose)	7th (I1)	Complete absence of acute inflammation, negligible disruption in epithelial cells
		14th (I2)	Mucosa appears normal; Absence of lesions indicating pathological significance

group 8 and 9 as compared to the group 1 (normal control $p > 0.05$). This was followed by rats of group 7 who received treatment of combination of MAP and MES as compared to rats of group 3 to group 6. MES is first line drug to treat UC and MAP has also been reported for its anti-ulcer potential (REF). Hence, co-administration of these two have shown better anti-ulcer potential as that of MAP alone (group 3), MES alone (group 4) and AgNPs at both doses (groups 5 and 6). The decreasing order of MPO level on 7th and 14th days was in the following order:

group 2 > group 3 > group 4 > group 5 > group 6 > group 7 > group 8 > group 9 > group 1

The levels for TBARs and TNF-α for various treatment groups were found same as that of MPO whereas, the levels of GSH and SOD were found opposite to that of MPO (Fig. 6b–e). The decreasing order of GSH and SOD was found in the following order:

group 1 > group 9 > group 8 > group 7 > group 6 > group 5 > group 4 > group 3 > group 2

The result of these parameters also indicated that the combination treatment of MAP, MES and AgNPs was able to reduce the inflammation of the intestine successfully [51].

3.2.5.1. Estimation of treatment on the colonic weight ratio in acetic acid induced UC rat model. The colonic weight ratio was determined for isolated colon of all the groups (group1 to group 8) that were sacrificed on 7th and 14th day respectively. There was a significant increase ($P < 0.001$) in the colonic weight ratio for the rats from the group 2 to group 7 as compared to the group 1. However, the weight ratios of the colons of the rats of group 8 and 9 were found closer to the group 1. It was very important to notice that more colonic weight ratio signifies more inflammation to colonic and more damage. The colonic weight ratios of the different groups were found in the following increasing order on 7th as well as 14th days (Fig. 7a).

group 1 < group 9 < group 8 < group 7 < group 6 < group 5 < group 4 < group 3 < group 2

3.2.5.2. Estimation of disease activity index (DAI). DAI score was determined on 0^{th}, 7th, and 14th day of the study in the treatment groups. To evaluate DAI, each of the individual scores of the parameters like percentage loss of weight and consistency of stool were determined. The overall DAI for individual rat was determined by addition of individual scores followed by dividing the total score by two. The interpretations of overall DAI for different groups are shown in Fig. 7b–d. The day of administering acetic acid through the rectal route is considered as day 0 and hence no sign of UC was observed. On the 7th day after the induction of UC, experimental control group (group 2) animals suffered the maximum % weight loss. Thus, this group showed a significant rise in the DAI score as compared to normal control (group 1) with $p < 0.001$. But a significant difference was seen in the DAI score when group 2 was compared with group 8 and group 9 ($p < 0.001$) and group 3 and group 4 ($p < 0.05$). On the 14th day of the study, the stool consistency in groups 8 and 9 were normal. The DAI score revealed that group 8 and group 9 did not have any significant difference with group 1 (normal control) with $p > 0.001$ whereas, group 3 and group 4 showed a significant difference as compared to group 2 ($p < 0.001$). The rats of groups 5 and 6 who received only AgNPs treatment have also shown better recovery, however, it was significantly less ($p < 0.05$) as that of groups 8 and 9, indicating the potential of co-administration of MES with AgNPs.

The value of DAI score is directly proportional with the severity of the disease [52,53]. The score was maximum in case of group 2 and minimum in group 1 after two days of the induction of the disease. A treatment regime of 14 days was provided to the UC induced rats. All the groups showed a certain level of reduction in the DAI score after the complete treatment regime and followed the following pattern of reduction:

group 9 > group 8 > group 7 > group 6 > group 5 > group 4 > group 3, which confirmed the efficacy of the combined dose of MAP, MES and AgNPs over their single treatment regime.

3.2.5.3. Histopathological examination. Microscopic examination of all the isolated tissue was carried out and the details of histopathological impressions are shown in Table 3 and images are shown in Figs. 8 and 9. The result of the histopathological study supports the results of DAI and other parameters of UC treatment obtained in the entire study.

4. Conclusion

The present investigation indicated the potential effect of co-administration of AgNPs with MES and MAP against acetic acid induced rat model for ulcerative colitis. The study clearly indicated dual role of MAP since it helped in reduction of $AgNO_3$ for production of AgNPs and acted as anti-oxidant and anti-ulcer agent as well. The AgNPs

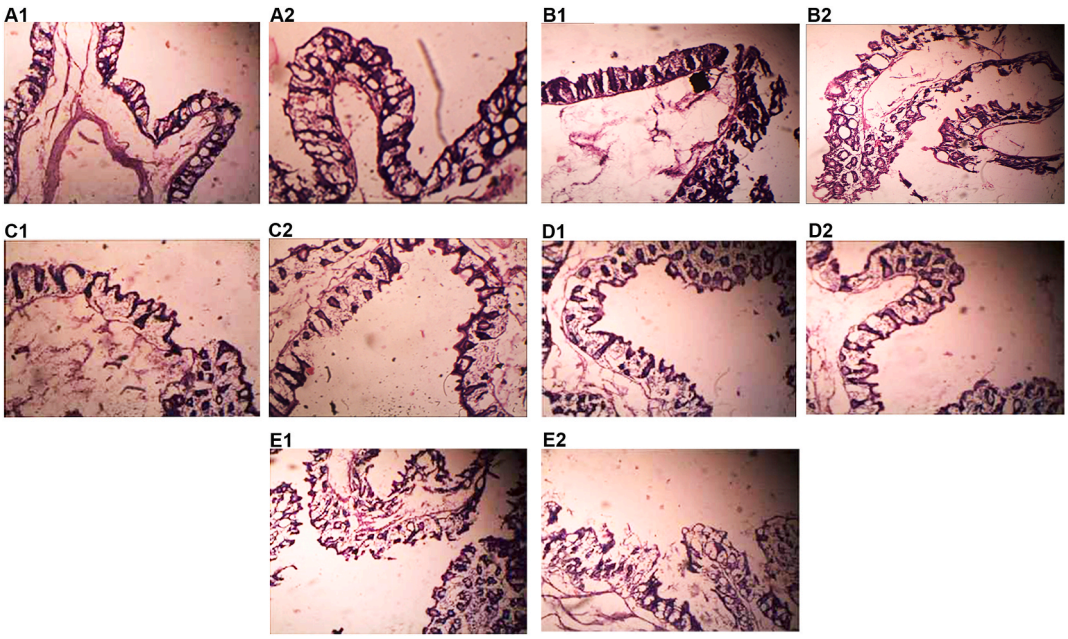

Fig. 8. Histopathological images of colonic tissues of rats of group 1 (A), group 2 (B), group 3 (C), group 4 (D) and group 5 (E). Note: Numeric 1 shows histopathology of rats' colon on day 7 and numeric 2 represents histopathology of rats' colon on day 14. Image taken using x 40 lens.

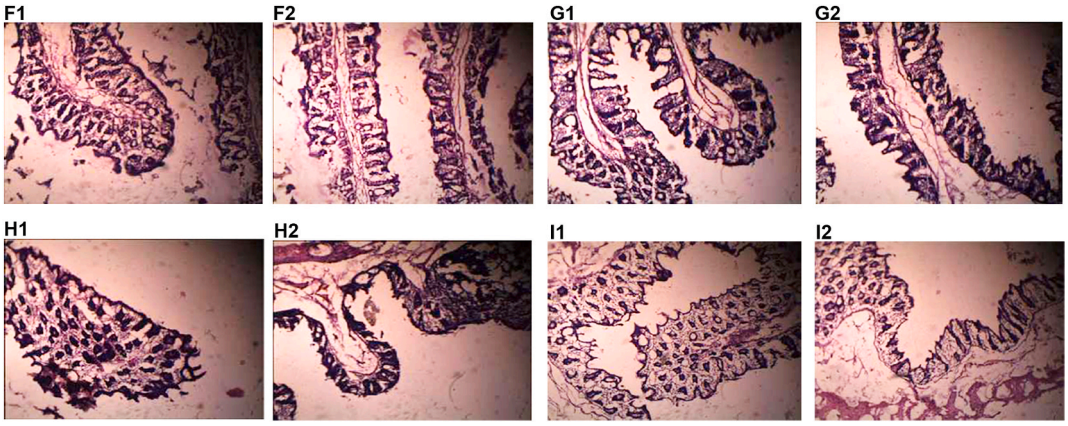

Fig. 9. Histopathological images of colonic tissues of rats of group 6 (F), group 7 (G), group 8 (H) and group 9 (I) on day 7 and 14. Note: Numeric 1 shows histopathology of rats' colon on day 7 and numeric 2 represents histopathology of rats' colon on day 14. Image taken using x 40 lens.

were developed using MAP dissolved in citrate buffer and characterized through DLS, SPR and TEM. The dissolution study of MES in AgNPs-MES provided restriction of about 50% of drug in the upper GIT and targeted rest of them to the colonic site. The *in-vivo* biochemical and histopathological studies supported the drug targeting effect because the combination of MAP, MES and AgNPs (groups 8 and 9) provided better efficacy to treat UC as compared to their individual treatment.

CRediT authorship contribution statement

Gurmandeep Kaur: Methodology, Data curation, Writing - original draft. **Sachin Kumar Singh:** Conceptualization, Validation, Supervision, Writing - review & editing. **Rajesh Kumar:** Supervision. **Bimlesh Kumar:** Supervision. **Yogita Kumari:** Methodology. **Monica Gulati:** Supervision, Writing - review & editing. **Narendra Kumar Pandey:** Methodology. **K. Gowthamarajan:** Methodology. **Dipanjoy Ghosh:** Methodology. **A. Clarisse:** Methodology. **Sheetu Wadhwa:** Methodology. **Meenu Mehta:** Methodology. **Saurabh Satija:** Methodology. **Kamal Dua:** Validation. **Harish Dureja:** Methodology. **Saurabh Gupta:** Methodology. **Pankaj Kumar Singh:** Methodology. **Bhupinder Kapoor:** Methodology. **Nitin Chitranshi:** Methodology. **Ankit Kumar:** Methodology. **Omji Porwal:** Methodology.

Declaration of competing interest

The authors declare that they have no known competing financial interests or personal relationships that could have appeared to influence the work reported in this paper.

References

[1] S. Alatab, S.G. Sepanlou, K. Ikuta, H. Vahedi, C. Bisignano, S. Safiri, A. Sadeghi, M. R. Nixon, A. Abdoli, H. Abolhassani, The global, regional, and national burden of inflammatory bowel disease in 195 countries and territories, 1990–2017: a systematic analysis for the Global Burden of Disease Study 2017, Lancet Gastroenterol. Hepatol. 5 (2020) 17–30.

[2] M.A. Al-Shamali, M. Kalaoui, I. Patty, F. Hasan, A. Khajah, B. Al-Nakib, Ulcerative colitis in Kuwait: a review of 90 cases, Digestion 67 (2003) 218–224.

[3] E.I. Benchimol, D.R. Mack, A. Guttmann, G.C. Nguyen, T. To, N. Mojaverian, P. Quach, D.G. Manuel, Inflammatory bowel disease in immigrants to Canada and

their children: a population-based cohort study, Am. J. Gastroenterol. 110 (2015) 553.
[4] S. Kedia, V. Ahuja, Epidemiology of inflammatory bowel disease in India: the great shift east, Inflamm. Intesti. Dis. 2 (2017) 102–115.
[5] A.E. M'koma, Inflammatory bowel disease: an expanding global health problem, Clin. Med. Insights Gastroenterol. 6 (2013). CGast. S12731.
[6] S.C. Ng, W. Tang, J.Y. Ching, M. Wong, C.M. Chow, A. Hui, T. Wong, V.K. Leung, S. W. Tsang, H.H. Yu, Incidence and phenotype of inflammatory bowel disease based on results from the Asia-pacific Crohn's and colitis epidemiology study, Gastroenterology 145 (2013) 158–165, e152.
[7] Y. Niv, G. Abuksis, G.M. Fraser, Epidemiology of ulcerative colitis in Israel: a survey of Israeli kibbutz settlements, Am. J. Gastroenterol. 95 (2000) 693.
[8] C. Probert, V. Jayanthi, D. Pinder, A. Wicks, J. Mayberry, Epidemiological study of ulcerative proctocolitis in Indian migrants and the indigenous population of Leicestershire, Gut 33 (1992) 687–693.
[9] A. Tezel, G. Dökmeci, M. Eskiocak, H. Ümit, A. Soylu, Epidemiological features of ulcerative colitis in Trakya, Turkey, J. Int. Med. Res. 31 (2003) 141–148.
[10] S. Garud, M.A. Peppercorn, Ulcerative colitis: current treatment strategies and future prospects. therapeutic advances in gastroenterology 2 (2009) 99–108.
[11] S. Mohanta, S.K. Singh, B. Kumar, M. Gulati, R. Kumar, A.K. Yadav, S. Wadhwa, J. Jyoti, S. Som, K. Dua, Efficacy of co-administration of modified apple polysaccharide and probiotics in guar gum-Eudragit S100 based mesalamine mini tablets: a novel approach in treating ulcerative colitis, Int. J. Biol. Macromol. 126 (2019) 427–435, https://doi.org/10.1016/j.ijbiomac.2018.12.154.
[12] J. Panes, I. Alfaro, New treatment strategies for ulcerative colitis, Expet Rev. Clin. Immunol. 13 (2017) 963–973.
[13] G. Prudhviraj, Y. Vaidya, S.K. Singh, A.K. Yadav, P. Kaur, M. Gulati, K. Gowthamarajan, Effect of co-administration of probiotics with polysaccharide based colon targeted delivery systems to optimize site specific drug release, Eur. J. Pharm. Biopharm. 97 (2015) 164–172.
[14] M. World, P. Stevens, M. Ashton, D. Rainford, Mesalazine-associated interstitial nephritis, Nephrol. Dial. Transplant. 11 (1996) 614–621.
[15] M. Gohel, R. Parikh, S. Nagori, M. Dabhi, Design of a potential colonic drug delivery system of mesalamine, Pharmaceut. Dev. Technol. 13 (2008) 447–456.
[16] L. Jin, Y.-c. Ding, Y. Zhang, X.-q. Xu, Q. Cao, A novel pH–enzyme-dependent mesalamine colon-specific delivery system, Drug Des. Dev. Ther. 10 (2016) 2021.
[17] R. Kaur, M. Gulati, S.K. Singh, Role of synbiotics in polysaccharide assisted colon targeted microspheres of mesalamine for the treatment of ulcerative colitis, Int. J. Biol. Macromol. 95 (2017) 438–450.
[18] N.G. Kotla, M. Gulati, S.K. Singh, A. Shivapooja, Facts, fallacies and future of dissolution testing of polysaccharide based colon-specific drug delivery, J. Contr. Release 178 (2014) 55–62.
[19] A. Sharma, B. Kumar, S.K. Singh, M. Gulati, Y. Vaidya, H. Rathee, D. Ghai, A. H. Malik, A.K. Yadav, P. Maharshi, In-vitro and in-vivo pharmacokinetic evaluation of guar gum-eudragit® S100 based colon-targeted spheroids of sulfasalazine Co-administered with probiotics, Curr. Drug Deliv. 15 (2018) 367–387.
[20] P. Maharshi, S.K. Singh, M. Gulati, A.K. Yadav, V. Garg, B. Kumari, K. Gowthamarajan, A novel three-pronged approach for colon delivery of sulfasalazine: concomitant use of pH-responsive, microbially triggered polymers and liquisolid technology, Curr. Drug Deliv. 15 (2018) 1038–1054.
[21] S.K. Singh, A.K. Yadav, G. Prudhviraj, M. Gulati, P. Kaur, Y. Vaidya, A novel dissolution method for evaluation of polysaccharide based colon specific delivery systems: a suitable alternative to animal sacrifice, Eur. J. Pharmaceut. Sci. 73 (2015) 72–80.
[22] M. Kaur, A. Singh, B. Kumar, S.K. Singh, A. Bhatia, M. Gulati, T. Prakash, P. Bawa, A.H. Malik, Protective effect of co-administration of curcumin and sildenafil in alcohol induced neuropathy in rats, Eur. J. Pharmacol. 805 (2017) 58–66.
[23] K.C. Bhol, P.J. Schechter, Effects of nanocrystalline silver (NPI 32101) in a rat model of ulcerative colitis, Dig. Dis. Sci. 52 (2007) 2732–2742.
[24] Y. Li, L. Fan, T. Tang, Y. Tang, M. Xie, X. Zeng, Y. Sun, Q. Mei, Modified apple polysaccharide prevents colitis through modulating IL-22 and IL-22BP expression, Int. J. Biol. Macromol. 103 (2017) 1217–1223.
[25] K. Siczek, H. Zatorski, A. Chmielowiec-Korzeniowska, J. Pulit-Prociak, M. Śmiech, R. Kordek, L. Tymczyna, M. Banach, J. Fichna, Synthesis and evaluation of anti-inflammatory properties of silver nanoparticle suspensions in experimental colitis in mice, Chem. Biol. Drug Des. 89 (2017) 538–547.
[26] Y. Li, L. Liu, Y. Niu, J. Feng, Y. Sun, X. Kong, Y. Chen, X. Chen, H. Gan, S. Cao, Modified apple polysaccharide prevents against tumorigenesis in a mouse model of colitis-associated colon cancer: role of galectin-3 and apoptosis in cancer prevention, Eur. J. Nutr. 51 (2012) 107–117.
[27] Y. Kumari, S.K. Singh, R. Kumar, B. Kumar, G. Kaur, M. Gulati, D. Tewari, K. Gowthamarajan, V.N.R. Karri, C. Ayinkamiye, Modified apple polysaccharide capped gold nanoparticles for oral delivery of insulin, Int. J. Biol. Macromol. 149 (2020) 976–988, https://doi.org/10.1016/j.ijbiomac.2020.01.302.
[28] M. Chaurasia, M.K. Chourasia, N.K. Jain, A. Jain, V. Soni, Y. Gupta, S.K. Jain, Cross-linked guar gum microspheres: a viable approach for improved delivery of anticancer drugs for the treatment of colorectal cancer, AAPS Pharm. Sci. Tech 7 (2006) E143.
[29] Y. Krishnaiah, P.V. Raju, B.D. Kumar, V. Satyanarayana, R. Karthikeyan, P. Bhaskar, Pharmacokinetic evaluation of guar gum-based colon-targeted drug delivery systems of mebendazole in healthy volunteers, J. Contr. Release 88 (2003) 95–103.
[30] Y. Krishnaiah, P.B. Reddy, V. Satyanarayana, R. Karthikeyan, Studies on the development of oral colon targeted drug delivery systems for metronidazole in the treatment of amoebiasis, Int. J. Pharm. 236 (2002) 43–55.
[31] Y. Krishnaiah, V. Satyanarayana, B.D. Kumar, R. Karthikeyan, In vitro drug release studies on guar gum-based colon targeted oral drug delivery systems of 5-fluorouracil, Eur. J. Pharmaceut. Sci. 16 (2002) 185–192.
[32] Y. Krishnaiah, V. Satyanarayana, B.D. Kumar, R. Karthikeyan, P. Bhaskar, In vivo pharmacokinetics in human volunteers: oral administered guar gum-based colon-targeted 5-fluorouracil tablets, Eur. J. Pharmaceut. Sci. 19 (2003) 355–362.
[33] F. Li-Fang, H. Wei, C. Yong-Zhen, X. Bai, D. Qing, W. Feng, Q. Min, C. De-Ying, Studies of chitosan/Kollicoat SR 30D film-coated tablets for colonic drug delivery, Int. J. Pharm. 375 (2009) 8–15.
[34] L. Liu, Z.-P. Wang, C.-T. Xu, B.-R. Pan, Q.-B. Mei, Y. Long, J.-Y. Liu, S.-Y. Zhou, Effects of Rheum tanguticum polysaccharide on TNBS-induced colitis and CD4+ T cells in rats, World J. Gastroenterol. 9 (2003) 2284.
[35] V. Garg, P. Kaur, S.K. Singh, B. Kumar, P. Bawa, M. Gulati, A.K. Yadav, Solid self-nanoemulsifying drug delivery systems for oral delivery of polypeptide-k: formulation, optimization, in-vitro and in-vivo antidiabetic evaluation, Eur. J. Pharmaceut. Sci. 109 (2017) 297–315.
[36] L. Yang, Biorelevant dissolution testing of colon-specific delivery systems activated by colonic microflora, J. Contr. Release 125 (2008) 77–86.
[37] R. Fabia, R. Willen, A. Ar'Rajab, R. Andersson, B. Ahren, S. Bengmark, Acetic acid-induced colitis in the rat: a reproducible experimental model for acute ulcerative colitis, Eur. Surg. Res. 24 (1992) 211–225.
[38] L. Zhao, H. Wu, A. Zhao, H. Lu, W. Sun, C. Ma, Y. Yang, X. Xin, H. Zou, M. Qiu, The in vivo and in vitro study of polysaccharides from a two-herb formula on ulcerative colitis and potential mechanism of action, J. Ethnopharmacol. 153 (2014) 151–159.
[39] M. Hu, Measurement of protein thiol groups and GSH in plasma, in: L. Parker (Ed.), Methods in Enzimology, Academic Press, San Diego, 1990.
[40] S. Mohanta, S.K. Singh, B. Kumar, M. Gulati, R. Kumar, A.K. Yadav, S. Wadhwa, J. Jyoti, S. Som, K. Dua, Efficacy of co-administration of modified apple polysaccharide and probiotics in guar gum-Eudragit S100 based mesalamine mini tablets: a novel approach in treating ulcerative colitis, Int. J. Biol. Macromol. 126 (2019) 427–435.
[41] A. Shalaby, A. Shatta, Potential antioxidant and anti-inflammatory effects of Hyphaena thebaica in experimentally induced inflammatory bowel disease, Int. J. Pharmacol. Res. 9 (2013) 51–60.
[42] S. Das, L. Kanodia, Effect of ethanolic extract of leaves of Moringa olifera lam. on acetic acid induced colitis in albino rats, Asian J. Pharmaceut. Clin. Res. 5 (2012) 110–114.
[43] V.P. Shah, Y. Tsong, P. Sathe, J.-P. Liu, In vitro dissolution profile comparison—statistics and analysis of the similarity factor, f2, Pharmaceut. Res. 15 (1998) 889–896.
[44] S. Mohanta, S.K. Singh, B. Kumar, M. Gulati, J. Jyoti, S. Som, S. Panchal, I. Melkani, M. Banerjee, S.K. Sinha, Solidification of liquid Modified Apple Polysaccharide by its adsorption on solid porous carriers through spray drying and evaluation of its potential as binding agent for tablets, Int. J. Biol. Macromol. 120 (2018) 1975–1998.
[45] K.L. Kelly, E. Coronado, L.L. Zhao, G.C. Schatz, The Optical Properties of Metal Nanoparticles: the Influence of Size, Shape, and Dielectric Environment, ACS Publications, 2003.
[46] K.-S. Lee, M.A. El-Sayed, Gold and silver nanoparticles in sensing and imaging: sensitivity of plasmon response to size, shape, and metal composition, J. Phys. Chem. B 110 (2006) 19220–19225.
[47] L. Huang, M.L. Zhai, D.W. Long, J. Peng, L. Xu, G.Z. Wu, J.Q. Li, G.S. Wei, UV-induced synthesis, characterization and formation mechanism of silver nanoparticles in alkalic carboxymethylated chitosan solution, J. Nanoparticle Res. 10 (2008) 1193–1202.
[48] S.H. Lee, B.-H. Jun, Silver nanoparticles: synthesis and application for nanomedicine, Int. J. Mol. Sci. 20 (2019) 865.
[49] M.A. Mohammed, J. Syeda, K.M. Wasan, E.K. Wasan, An overview of chitosan nanoparticles and its application in non-parenteral drug delivery, Pharmaceutics 9 (2017) 53.
[50] G. Saravanakumar, D.-G. Jo, J.H. Park, Polysaccharide-based nanoparticles: a versatile platform for drug delivery and biomedical imaging, Curr. Med. Chem. 19 (2012) 3212–3229.
[51] X. Luo, A. Morrin, A.J. Killard, M.R. Smyth, Application of nanoparticles in electrochemical sensors and biosensors, Electroanalysis: Int. J. Devote. Fund. Practical. Aspects. Electroanalysis 18 (2006) 319–326.
[52] A. Algaba, P.M. Linares, M.E. Fernández-Contreras, A. Ordoñez, J. Trápaga, I. Guerra, M. Chaparro, G. de la Poza, J.P. Gisbert, F. Bermejo, Relationship between levels of angiogenic and lymphangiogenic factors and the endoscopic, histological and clinical activity, and acute-phase reactants in patients with inflammatory bowel disease, J. Crohn's Colitis 7 (2013) e569–e579.
[53] F. Ke, P.K. Yadav, L.Z. Ju, Herbal medicine in the treatment of ulcerative colitis, Saudi J. Gastroenterol.: Offi. J. Saudi Gastroenterol. Assoc. 18 (2012) 3.